Recruitment of human eIF4G1 or DAP5 to the 5' untranslated regions of a subset of cellular mRNAs drives cap-independent translation

Solomon A. Haizel[a,b], Usha Bhardwaj[b], Ruben L. Gonzalez Jr.[c], Somdeb Mitra[c,d], and Dixie J. Goss[a,b,e,f]

[a] *Ph.D. Program in Biochemistry, The Graduate Center of the City University of New York, New York, NY 10016*
[b] *Department of Chemistry, Hunter College, New York, NY 10065*
[c] *Department of Chemistry, Columbia University, New York, NY 10027*
[d] *Department of Chemistry, New York University, New York, NY 10003*
[e] *Ph.D. Program in Chemistry, The Graduate Center of the City University of New York, New York, NY 10016*

[f] To whom correspondence may be addressed: Dixie J. Goss, Department of Chemistry, Hunter College, New York, NY 10065, USA, Tel.: (212) 772-5383; FAX: (212) 772-5332; Email: dgoss@hunter.cuny.edu

Abstract

During unfavorable cellular conditions (*e.g.*, tumor hypoxia, viral infection, nutrient deprivation, *etc.*), the canonical, cap-dependent translation initiation pathway in human cells is suppressed by sequestration of the cap-binding protein, eukaryotic initiation factor (eIF) 4E, by 4E-binding proteins. Additionally, the expression levels of eIF4G and its cellular homolog, death associated protein 5 (DAP5), are elevated. Under these conditions, a subset of cellular mRNAs, including many encoding proteins with important roles in human health and disease, (e.g. HIF-1α, FGF-9, and p53) is translated in a cap-independent manner. Despite their physiological importance, however, the molecular mechanisms underlying cap-independent initiation of this subset of cellular mRNAs remain unknown. Here, we have used fluorescence anisotropy-based equilibrium binding assays developed in our laboratories to demonstrate that an N-terminal truncated form of human eIF4G1 that cannot interact with eIF4E (ΔN-4G1) or DAP5 directly bind to the 5' untranslated regions (UTRs) of these mRNAs. Specifically, we have measured the differential affinities with which ΔN-4G1 and DAP5 interact with the 5' UTRs of four distinct members of this subset of cellular mRNAs. Using a luciferase-based gene expression reporter assay, we further demonstrate that these same 5' UTRs can promote cap-independent initiation in an ΔN-4G1 or DAP5-dependent manner in a rabbit reticulocyte lysate-based *in vitro* translation system. Integrating the results of our quantitative binding- and *in vitro* translation studies, we propose a model specifying how a subset of cellular mRNAs switch from cap-dependent to cap-independent modes of translation initiation

Keywords

5' CITE | eIF4FG | DAP5 | fluorescence anisotropy

Significance

Under cellular stress conditions (e.g., tumor hypoxia, viral infection, etc.), the canonical, cap-dependent initiation of eukaryotic protein synthesis, or translation, of a subset of cellular mRNAs switches to a cap-independent mechanism. Despite the important role they play in human health and disease, the mechanisms regulating this switch remain unknown. We have found that a variant of eukaryotic initiation factor (eIF) 4G1 and its homolog, DAP5, factors that are upregulated under stress conditions, bind with high affinity and specificity to the 5' untranslated regions of these mRNAs and upregulate their translation. These results suggest that binding of

eIF4G1 or DAP5 to these mRNAs plays an important role in regulating the switch between the cap-dependent and cap-independent initiation of these mRNAs.

Introduction

Translation of mRNAs into proteins is the most energy consuming process in the cell and plays a major role in the regulation of gene expression. In eukaryotes, translation initiation of cellular mRNAs generally occurs *via* a 'cap-dependent' pathway in which eukaryotic initiation factor (eIF) 4E binds to the N7-methylguanosine-triphosphate 'cap' at the 5' end of the mRNA to be translated (1, 2). Cap-bound eIF4E subsequently recruits eIF4G, which, together with eIF4A, recruit a ribosomal 43S pre-initiation complex (PIC) composed of the small, 40S, ribosomal subunit, a methionylated initiator transfer RNA (Met-tRNA$_i^{Met}$), and additional eIFs. Subsequent scanning of the resulting 48S PIC to find the AUG start codon on the mRNA and joining of the 60S ribosomal subunit to the 48S PIC result in the formation of an elongation competent 80S IC that can go on to translate the mRNA.

In addition to undergoing cap-dependent initiation, certain classes of cellular mRNAs can also initiate *via* 'cap-independent' pathways in response to cellular conditions. The ability of these mRNAs to switch from cap-dependent to cap-independent modes of initiation plays an important role in maintaining normal cellular physiology (3) as well as in the cellular response to diseases such as cancer, diabetes, and, possibly, neurological disorders (4-9). One class of cellular mRNAs, for example, has been shown to successfully bypass a global suppression of initiation that is caused by stress conditions such as tumor hypoxia, viral infection, nutrient deprivation, *etc.* (1, 10-12) and that is driven by the sequestration of eIF4E by hypophosphorylated 4E-binding proteins (4E-BPs). These mRNAs, many of which encode proteins such as hypoxia inducing factor 1α (HIF-1α), fibroblast growth factor 9 (FGF-9), and the p53 tumor suppressor protein (p53) that play important roles in human health and disease, contain highly stable structures in their 5' untranslated regions (UTRs) that act as 'cap-independent translation enhancers' (CITEs) (11, 13).

Although the ability of CITE-containing mRNAs (hereafter referred to as CITE-mRNAs) to bypass the 4E-BP-mediated global suppression of cap-dependent initiation has been linked to enhanced tumor development and cancer progression(14), details of the process through which CITE-mRNAs switch from cap-dependent to cap-independent modes of translation initiation under these conditions and the extent to which initiation of CITE-mRNAs is actually cap and/or eIF4E independent are not clear. One proposal describing how CITE-mRNAs are preferentially translated under stress conditions posits that CITE-mRNAs outcompete non-CITE-mRNAs in the recruitment of limiting amounts of eIFs (15, 16). Consistent with this proposal, many of the stress conditions that result in suppression of cap-dependent initiation also result in increased expression levels of eIF4G (4, 5) and/or death associated protein 5 (DAP5) (17, 18) suggesting these two proteins may be involved in the cap-independent initiation of CITE-mRNAs. DAP5 is homologous to the C-terminal two-thirds of eIF4G and is abundantly expressed in proliferating cells (18-20). Consistent with its homology to eIF4G, DAP5 interacts with eIF4A and the eIF3 component of the 43S PIC. Notably, however, DAP5 lacks the N-terminal, eIF4E-binding domain that is present in eIF4G and, consequently, does not interact with eIF4E. As such, DAP5 does not play a role in cap-dependent initiation and has instead been shown to mediate the cap-independent translation of a number of CITE-mRNAs, including the p53 CITE-mRNA (21). There have been no systematic quantitative studies to show the direct recruitment of DAP5 or eIF4G to CITE-mRNA and how such recruitment might distinguish among CITE-mRNAs or drive the switch from cap-dependent to cap-independent initiation in response to cellular stress.

To address these gaps in our understanding, we have developed and used a fluorescence anisotropy-based equilibrium binding assay to measure the affinities with which a variant of human eIF4G1 that lacks the N-terminal, eIF4E-binding domain (ΔN-4G1) and human

DAP5 bind to oligonucleotides corresponding to the 5' UTRs of a representative set of CITE-mRNAs (CITE-UTRs), namely the HIF-1α, FGF-9, and p53 CITE-UTRs. Complementing these binding assays, we have developed and used a luciferase-based gene expression reporter assay to characterize whether and to what extent binding of ΔN-4G1 and DAP5 promotes the initiation and translation of luciferase-encoding mRNAs containing these same CITE-UTRs, hereafter referred to as CITE-Luc mRNAs, in a rabbit reticulocyte lysate-based *in vitro* translation system in which cap-dependent initiation has been largely abrogated. The results of our experiments demonstrate that ΔN-4G1 and DAP5 exhibit differential binding affinities to the HIF-1α, FGF-9, and p53 CITE-UTRs that correlate with the differential abilities of these eIFs to drive the initiation and translation of these CITE-Luc mRNAs. Based on our collective results, we propose a model for how CITE-mRNAs regulate the switch from cap-dependent to cap-independent initiation and drive expression of the proteins they encode in response to cellular stress.

Results

ΔN-4G1 and DAP5 bind to the CITE-UTRs with affinities that vary among CITE-UTRs and between the two translation factors

To characterize the binding of ΔN-4G1 and DAP5 to the HIF-1α, FGF-9, and p53 CITE-UTRs, we developed a fluorescence anisotropy-based equilibrium binding assay (Fig. 1). This assay reports on the fluorescence anisotropy of a fluorescein fluorophore that is covalently attached to the 5' terminus of the HIF-1α and FGF-9 CITE-UTRs and the two p53 CITE-UTRs corresponding to CITE elements in the 5' UTR and within the coding region, respectively, of the p53 mRNA (hereafter referred to as the $p53_A$ and $p53_B$ CITE-UTRs) and lacking a 5' N7-methylguanosine triphosphate cap. In this assay, binding of ΔN-4G1 or DAP5 to the fluorescein-labeled CITE-UTRs results in an increase in the molecular weight of the CITE-UTRs that is expected to increase the rotational time, and, consequently, the fluorescence anisotropy, of the fluorescein reporter. To quantify the affinity of ΔN-4G1 and DAP5 binding to the four CITE-UTRs, we recorded the change in the fluorescence anisotropy of each fluorescein-labeled CITE-UTR as a function of increasing concentrations of ΔN-4G1 or DAP5 and fitted the resulting data points with a single-site equilibrium binding isotherm (Fig. 2A and 2B). The results of these experiments, which are reported in Table 1, demonstrate that ΔN-4G1 and DAP5 bind to the four CITE-UTRs with equilibrium dissociation constants (K_ds) ranging from 102–300 nM.

Comparative analyses of our results demonstrate that ΔN-4G1 and DAP5 exhibit differential binding affinities both among the CITE-UTRs and between the two translation factors. Specifically, the K_d for ΔN-4G1 binding to the $p53_B$ CITE-UTR is more than 2-fold lower than the K_d for ΔN-4G1 binding to the $p53_A$ and FGF-9 CITE-UTRs (Table 1). DAP5 exhibited an even greater difference in binding affinity among the CITE-UTRs, with a K_d for binding to the FGF-9 CITE-UTR that is more than 2.5-fold lower than the K_d for binding to the $p53_A$ CITE-UTR. The difference in binding affinities between the two translation factors was also striking. The K_d for DAP5 binding to the FGF-9 CITE-UTR, for example, is almost 2-fold lower than the K_d of ΔN-4G1 binding to the same CITE-UTR. Contrasting with this, the K_d for ΔN-4G1 binding to the $p53_B$ CITE-UTR is more than 2-fold lower than the K_d of DAP5 binding to the same CITE-UTR.

Binding of ΔN-4G1 and DAP5 is specific for particular sequence elements in the CITE-UTRs.

Given previous studies demonstrating that CITE-mRNAs contain highly stable structures in their 5' UTRs (2,9) and proposals that CITE-mRNAs might function by outcompeting non-CITE-mRNAs in the recruitment of limiting amounts of eIFs (15, 16) such as eIF4G and DAP5, we conjectured that structural features within the 5' UTRs of the CITE-mRNAs might act as recognition elements and binding sites for ΔN-4G1 and DAP5. Nonetheless, examination of the sequences and predicted secondary structures of the 5' UTRs of the CITE-mRNAs did not lead

to identification of any obvious structural features that were common to all four 5' UTRs and that could serve as likely recognition elements and binding sites for ΔN-4G1 or DAP5. We therefore decided to investigate the specificity with which ΔN-4G1 and DAP5 interact with the 5' UTRs of the four CITE-mRNAs. In order to do this, we used our fluorescence anisotropy-based equilibrium binding assay to test the binding of ΔN-4G1 and DAP5 to a presumably unstructured, 101-nucleotide polyUC. The results of these experiments demonstrate that neither ΔN-4G1 or DAP5 exhibit appreciable binding to the polyUC oligonucleotide (Fig. 3), findings consistent with the hypothesis that structural features within the 5' UTRs of the CITE-mRNAs might act as recognition elements and binding sites for ΔN-4G1 and DAP5.

In order to more generally investigate how binding of ΔN-4G1 and DAP5 to RNA depends on structural features within the RNA and to contextualize and validate the results of the binding studies above, we used our fluorescence anisotropy-based equilibrium binding assay to investigate the binding of ΔN-4G1 and DAP5 to a series of RNAs either containing or lacking RNA structural elements that have been previously shown to act as recognition elements and binding sites for eIF4G and/or DAP5. Previously, we have shown that eIF4F binds to the 30-nucleotide iron responsive element (IRE) stem-loop within the 5' UTR of the mRNA encoding ferritin with a K_d of 9 nM, a binding interaction that stimulates ferritin mRNA translation in response to elevated cellular concentration of iron (22, 23). More importantly, we showed that eIF4F did not appreciably bind to a control, 30-nucleotide RNA stem-loop, highlighting the specificity with which eIF4F recognizes and binds the IRE. Using our fluorescence anisotropy-based equilibrium binding assay, here we show that ΔN-4G1 and DAP5 bind to the IRE with K_ds of 18 nM and 35 nM, respectively (Fig. S1). Similarly, we performed experiments in which we quantified the affinity of ΔN-4G1 and DAP5 for the J/K domain of the internal ribosomal entry site (IRES) in the 5' UTR of the mRNA encoding the encephalomyocarditis virus (EMCV) polyprotein (Fig. S1 and Table S1). These experiments show that ΔN-4G1 and DAP5 bind the EMCV J/K IRES with K_ds of 175 nM and 519 nM, respectively, values that are very similar to the K_d of 170 nM (24) that has been previously reported for the binding of human eIF4G1(643-1076) to the EMCV J/K IRES as part of the mechanism through which eIF4G1 drives expression of the EMCV polyprotein in human cells. The same report showed that an N-terminal piece of DAP5 (62-330) did not bind to the EMCV J/K IRES, consistent with our much higher K_d (519 nM) for full length DAP5 compared to ΔN-4G1 binding. As a further negative control for our CITE-UTR, IRE, and EMCV J/K IRES experiments, we attempted to quantify the affinity of ΔN-4G1 and DAP5 for the uncapped 5' UTR of mRNA encoding human β-actin (Fig. S1 and Table S1). These control experiments show that ΔN-4G1 and DAP5 do not appreciably bind uncapped β-actin mRNA, a result that is consistent with the previous and widespread use of this mRNA as a control for cap dependent initiation and translation (25).

ΔN-4G1 and DAP5 stimulate cap-independent in vitro translation of CITE-Luc mRNAs

In order to determine whether binding of ΔN-4G1 and DAP5 to the 5' UTRs of CITE-mRNAs can stimulate translation of these mRNAs, we developed a luciferase-based gene expression reporter assay and used it to characterize whether and to what extent ΔN-4G1 and DAP5 modulate CITE-mRNA expression. Briefly, the 5' UTRs of the HIF-1α, FGF-9, $p53_A$, and $p53_B$ CITE-mRNAs and as a control, the 5' UTR of β-actin mRNA were cloned upstream of a luciferase reporter gene and the resulting CITE-Luc mRNAs and β-act-Luc mRNA were translated using a rabbit reticulocyte lysate-based *in vitro* translation system in which cap-dependent initiation was suppressed through the addition of a 5' cap analog, m7G(5')ppp(5')G. Using this assay, we measured the luciferase activity produced by each translation reaction in the absence, as well as in the presence of increasing concentrations, of ΔN-4G1 and DAP5. The results of these experiments show that both ΔN-4G1 and DAP5 can significantly stimulate the cap-independent translation of all four CITE-Luc mRNAs by factors ranging between 2-fold to 5-fold over control reactions performed in the absence of the cap analog or added ΔN-4G1 or

DAP5 (Fig. 4). Specifically, ΔN-4G1 stimulates the HIF-1α, FGF-9, $p53_A$, and $p53_B$ CITE-Luc mRNAs by 5.1, 4.3, 3.6, and 4.6-fold, respectively, and DAP5 stimulates the HIF-1α, FGF-9, $p53_A$, and $p53_B$ CITE-Luc mRNAs by 3.9, 3.4, 2.6, and 2.3-fold, respectively (Table 2). Notably, the results also show that the concentration of ΔN-4G1 or DAP5 that exhibits the maximum stimulation varies both among the CITE-Luc mRNAs and between the two translation factors. Significantly, neither protein affected the translation of the control β-actin-Luc mRNA (Fig. S2 and Table 2) indicating the specificity of the stimulation.

Discussion

Using a fluorescence anisotropy-based equilibrium binding assay and a luciferase-based gene expression reporter assay, we have demonstrated that ΔN-4G1 and DAP5 bind to a representative set of CITE-UTRs with K_ds in the range of 102-300 nM (Fig. 2 and Table 1) and stimulate the cap-independent translation of the corresponding CITE-Luc mRNAs by 2-5 fold (Fig. 4 and Table 2). These K_ds are comparable to those observed for the binding of ΔN-4G1 and DAP5 to the IRE stem-loop and the EMCV J/K IRES (Fig.3, Fig. S1, Table 1, and Table S1), two systems in which it has been previously shown that binding of ΔN-4G1 to a well-defined structural feature within the 5' UTR of an mRNA can stimulates the cap-independent translation of the mRNA (23, 24). Highlighting the specificity of our results, we find that ΔN-4G1 and DAP5 exhibit negligible binding to a polyUC control oligonucleotide, and an uncapped control mRNA encoding β-actin (Fig. 3, Fig S1, Table 1, and Table S1) and, correspondingly, that ΔN-4G1 and DAP5 do not stimulate the cap-independent translation of the control mRNA encoding β-actin (Fig. S2 and Table 2). Together with the observation that ΔN-4G1 and DAP5 do not appreciably bind to our control RNAs, the observation that these translation factors bind to the CITE-UTRs studied here with affinities that are similar to those with which they bind the IRE stem-loop and the EMCV J/K IRES strongly suggests that ΔN-4G1 and DAP5 recognize and bind to specific structural features within the CITE-UTRs. Moreover, the observation that ΔN-4G1 and DAP5 exhibit different binding affinities both among the CITE-UTRs and between the two translation factors (Fig. 4 and Table 2) suggest that ΔN-4G1 and DAP5 differentially recognize different structural features in the various CITE-UTRs. The differential binding affinities of these two proteins for the CITE-UTRs observed here is in agreement with comparative structural studies showing distinct surface properties between the core domains of eIF4G and DAP5 isoforms from human and yeast systems (26).This observation may explain our inability to easily identify a consensus structural feature within the CITE-UTRs studied here that could serve as a likely recognition element and binding site for ΔN-4G1 and DAP5. Thus, the structural basis for ΔN-4G1 and DAP5 recognition and binding to specific sites within CITE-UTRs remains to be determined.

It is likely that the variations in the binding affinities described in the previous paragraph may underlie the variations we observe in the abilities of ΔN-4G1 and DAP5 to stimulate the cap-independent translation of the CITE-mRNAs studied here (Fig. 2 and Table 1). Indeed, with the exception of the $p53_B$ CITE-Luc mRNA, the extent to which ΔN-4G1 stimulates translation of these CITE-Luc mRNAs follows the same trend as that of the K_d for the binding of ΔN-4G1 to the corresponding CITE-UTRs (Fig. 2 and Table 1). Likewise, with the exception of the $p53_B$ CITE-Luc mRNA, the extent to which DAP5 stimulates translation of these CITE-Luc mRNAs follows the same trend as that of the K_d for the binding of DAP5 to the corresponding CITE-UTRs (Fig. 2 and Table 1). Given the close correlation between these trends, we hypothesize that binding of ΔN-4G1 and DAP5 to CITE-UTRs comprises an important aspect of the mechanism through which these translation factors stimulate the cap-independent translation of CITE-mRNAs. Moreover, the fact that the ΔN-4G1 or DAP5 concentration that exhibits the maximum stimulation of cap-independent translation for the CITE-Luc-mRNAs studied here varies both among the CITE-Luc-mRNAs and between the two translation factors

suggests that ΔN-4G1 and DAP5 may play complex roles in the recruitment of the 43S PIC and conversion of the 43S PIC to a 48S PIC.

Our findings are reminiscent of the manner in which viruses, such as EMCV, use highly structured IRESs to directly recruit eIFs, the 40S subunit, and/or the 43S PIC to drive the cap-independent translation of viral mRNAs (11, 27). Although the mechanisms through which viral mRNAs use IRESs to drive cap-independent initiation have been extensively characterized using genetic, biochemical, and structural approaches (13, 28, 29), the mechanisms through which eukaryotic cellular mRNAs drive cap-independent initiation remain largely unknown. Nonetheless, an increasing body of evidence suggests eukaryotic cellular mRNAs can employ non-canonical initiation mechanisms that are distinct from those employed by IRES-containing viral mRNAs. For example, Cate and co-workers have recently shown that the 'd' subunit of eIF3 (eIF3d) targets cell proliferation mRNAs and serves as a transcript specific cap-binding protein (30). Using the mRNA encoding the *c-Jun* transcription factor as an example, these authors showed that, under conditions in which an RNA structure in the 5' UTR blocks eIF4E from binding to the 5' cap, eIF3d binds directly to the 5' cap and serves as an alternative cap binding factor (31). Even more recently, it has been shown that DAP5 is a direct binding partner of eIF3d and it has been proposed that DAP5 used eIF3 to direct the eIF4E-independent cap-dependent translation of a subset of cellular mRNAs when cellular stress conditions lead to inactions of eIF4E (32). In addition to these mechanisms in which viral mRNAs possess IRES elements or eIF3d or other eIFs function as alternative cap-binding proteins, the methylation of adenosine residues in the 3'- and 5' UTRs of eukaryotic cellular mRNAs have been shown to stimulate translation by an unknown mechanism (33-35). The CITE-based mechanism we have investigated here is distinct from these other types of mechanisms in that, rather than making use of an alternative cap-binding protein or post-transcriptional modification of the mRNA to be translated, eIF4G1 or DAP5 completely bypass any cap-dependent processes and are instead directly recruited to CITEs within the 5' UTR of CITE-mRNAs. Indeed, because the binding studies we present here employ purified ΔN-4G1 and DAP5 and uncapped RNA oligonucleotides, our results show these translation factors can bind directly to CITE-mRNAs in a completely cap-independent manner and without the need of alternative cap-binding proteins. Similarly, because the gene expression assays we present here also employ purified, uncapped mRNAs and are performed in the presence of a cap analog, we can be confident that the stimulation of translation we observe is due to the direct interaction of ΔN-4G1 and DAP5 with the CITEs in the CITE-mRNAs, rather than to the indirect effects of alternative cap-binding proteins or methylation of the mRNA.

Given all of the above, we propose a model for the cap-independent initiation of eukaryotic cellular CITE-mRNAs that bears some similarities to the cap-independent initiation of IRES-containing viral mRNAs (36). Specifically, we propose that eIF4G1 or DAP5, perhaps with the aid of additional factors, bind to structural features within the CITEs of CITE-mRNAs and subsequently recruit additional eIFs, the 40S subunit, and/or the 43S PIC. In analogy to the cap-independent initiation of several IRES-containing viral mRNAs (36), we propose that the resulting 48S PIC may then scan to the AUG start codon and potentially establish interactions with RNA structural features and/or RNA-protein complexes at the 3' UTR of the CITE-mRNA that may further enhance expression (29, 37-39). This model provides an attractive mechanism through which CITE-mRNAs can bypass the canonical requirement for eIF4E and undergo cap-independent initiation and expression during cellular stress conditions.

Materials and Methods

Preparation of RNAs for fluorescence anisotropy-based equilibrium binding studies

DNA templats corresponding to the HIF-1α (ntds. 775-925, GenBank Accession Number: AH006957.2.) (40), FGF-9 (ntds 1233-1333, GenBank Accession Number: AY682094.1)(41), $p53_A$ (ntds. 158-191, GenBank Accession Number: JN900492.1) and $p53_B$ (ntds. 1-117, GenBank Accession Number: MG595994.1)(42) CITE-mRNAs, the ferritin IRE (22), the EMCV J/K IRES (ntds 680-786) (24, 43), and the full-length 5' UTR of β-actin (ntds. 1-84, GenBank Accession Number AK301372.1) (25) were purchased from Integrated DNA Technology (IDT) and *in vitro* transcribed using the HiScribe™ T7 Quick High Yield RNA synthesis Kit (New England Biolabs Inc.). RNA from transcription reactions were purified using the RNA Clean and Concentrator (RCC) Kit from Zymo Research following the manufacturer's protocol. Purified RNA transcripts were labeled with fluorescein at their 5' termini using the 5' EndTag DNA/RNA Labeling Kit from Vector Laboratories following the manufacturer's protocol.

Preparation of ΔN-4G1 and DAP5

A plasmid bearing a codon-optimized construct encoding human ΔN-4G1 (encompassing residues 682-1599 of human eIF4G1) (44) which includes the minimal sequence for IRES-mediated cap-independent translation initiation (24) was a generous gift form Dr. Christopher Fraser (University of California at Davis). This construct had an N-terminal, 6x-histidine tag followed by a Flag tag. A tobacco etch virus (TEV) protease cleavage site was introduced after the Flag tag, using Q5® Site Directed Mutagenesis Kit from New England Biolabs Inc. The plasmid encoding full length human DAP5 with an N-terminal 6x-histidine tag was purchased from Genscript (Piscataway, NJ). ΔN-4G1 and DAP5 were recombinantly expressed in *Escherichia coli* BL21-CodonPlus(DE3)-RIL cells (Agilent) and were purified using a combination of Ni^{2+}-nitro-tri-acetic acid (Ni-NTA) affinity and heparin affinity chromatography, as previously described (26, 45). Briefly, the proteins were first purified from bacterial cell lysates using His-Trap HP (Ni-NTA) columns (GE Healthcare life sciences), as per the manufacturer's instructions. The purified 6x-histidine tagged proteins were dialyzed overnight against Storage Buffer (20 mM HEPES pH 7.6, 200 mM KCl, 10 mM β-mercaptoethanol, 10% glycerol) in the presence of TEV protease to cleave off the tags. The untagged proteins were further purified and concentrated using 1 ml HiTrap™ Heparin HP columns (GE Healthcare life sciences). The eluted proteins were analyzed on 10% SDS-PAGE gels and pure fractions (>95% purity) were pooled and dialyzed overnight against Storage Buffer. The concentrations of the purified, concentrated proteins were quantified using Coomassie protein assay reagent (Thermo Scientific) and were aliquoted and stored at -80°C.

Fluorescence anisotropy-based equilibrium binding assays

Fluorescein-labeled RNAs were diluted t0 100 nM using Folding Buffer (20 mM HEPES pH 7.5 and 100 mM KCl) and heated to 90 °C for 2 mins and slowly cooled over 1 hr to room temperature. $MgCl_2$ to a final concentration of 1 mM was then added to the solution. The solution was then gently mixed and incubated on ice for about 1 hr. Fluorescence anisotropy measurements reporting on the binding of ΔN-4G1 or DAP5 to the fluorescein-labeled RNAs were performed using the equilibrium titration module of an SF-300X stopped-flow fluorimeter (KinTek Corporation, Austin, TX). Fluorescein-labeled RNAs were excited at 495 nm and emission was detected using a 515 nm high-pass filter (Semrock, Rochester, NY). Equilibrium binding titrations began with a 200 μl sample of 100 nM fluorescein-labeled RNA in Titration Buffer (20 mM HEPES, pH 7.6, 100 mM KCl, and 1 mM $MgCl_2$) and 50 data points were collected for each anisotropy measurement by automated continuous injection of 20 μl of ΔN-4G1 or DAP5 over a period of 30 min at a temperature of 25°C. Note that the first injection did

not contain any ΔN-4G1 or DAP5. Using the Origin 2018b software package, the data were fitted to a nonlinear, single-site, equilibrium binding equation of the form:

$$r_{obs} = r_{min} + (r_{max} - r_{min}) \left[\frac{[\Delta N-4G1 \text{ or } DAP5\,]}{Kd + [\Delta N-4G1 \text{ or } DAP5\,]}\right]$$

where r_{obs} is the observed anisotropy value, r_{min} is the minimum anisotropy value in the absence of ΔN-4G1 or DAP5, r_{max} is the final saturated anisotropy value, [ΔN-4G1 or DAP5] is the concentration of ΔN-4G1 of DAP5, and K_d is the equilibrium dissociation constant.
The chi-squared values (χ^2) that represented the statistical goodness of fit were always close to 1 and are reported in Table 1. The equilibrium binding titration of each CITE-UTR was performed three times and fit independently for K_d. The fitted K_ds were then averaged and the standard deviation calculated (Table 1).

Preparation of UTR-Luc reporter mRNAs for luciferase-based gene expression reporter assays.

The UTR-Luc mRNA constructs for the luciferase gene expression reporter assays were generated from the BlucB plasmid, (46) which contains a firefly luciferase gene flanked by 5'- and 3' UTR sequences of the Barley Yellow Dwarf Virus (BYDV) genomic RNA. To generate each UTR-Luc mRNA reporter construct, a sequences containing the T7 promoter followed by the target CITE-UTR was cloned into the BlucB plasmid vector upstream of the firefly luciferase coding region, after removing the BYDV 5' UTR. Briefly, all UTR-Luc reporter constructs were PCR amplified with NotI forward primer (CTAGGCGGCCGCTAATACGAC) and BssHII reverse primers(HIF1α:CTAGGCGCGCGGTGAATCGGTC, FGF9:CTAGGCGCGCCAGAGGACTCGGC, $p53_A$: CTAGGCGCGCGGCAGTGAC and $p53_B$: CTAGGCGCGCTGCTTGGGAC, and β-actin: CTAGGCGC GC GG TGAGCTGG) and then digested with NotI and BssHII. The PCR-amplified sequences were ligated into a NotI- and BssHII-digested BlucB plasmid using DNA ligase (New England Biolabs) and transformed into *E. coli* DH5-α competent cells. Five colonies were selected, grown overnight in Luria-Bertani (LB) growth media supplemented with 100 µg/mL ampicillin, and used to isolate plasmid DNA using the QIAprep® Spin Miniprep kit from Qiagen and following the manufacturer's protocol. All clones were confirmed by sequencing (Genewiz). To generate a linearized plasmid DNA template for *in vitro* transcription, plasmid DNA was linearized using Kpn1 so as to remove the 3' UTR from the CITE-Luc mRNA reporter construct and the resulting linearized DNA was purified using the GeneJET gel extraction and DNA cleanup Micro Kit from GeneJET and following the manufacurer's instructions. *In vitro* transcription reactions were preformed using the HiScribe™ T7 Quick High Yield RNA synthesis Kit kit from New England Biolabs Inc and following the manufacturer's protocol. NotI, BssHII, and KpnI were purchased from New England Biolabs and restriction digests were performed according to the manufacturer's instructions.

Luciferase-based gene expression reporter assays

Gene expression was achieved by *in vitro* translating the UTR-Luc mRNAs using the nuclease-treated rabbit reticulocytes lysate (RRL) *in vitro* translation system from Promega. Each 25 µl reaction contained 70% v/v of RRL, 0.02 mM amino acid mixture, 0.5 U/µl rRNAsin (Promega), 0.2 mM m7G(5')ppp(5')G cap-analog (Ambion), and varying concentrations of ΔN-4G1 or DAP5 as indicated in the figure legends. Briefly, 100 nM of UTR-Luc mRNA was added to a RRL *in vitro* translation mixture that had been pre-incubated at 30 °C for 10 mins following the addition of the specified concentration of ΔN-4G1 or DAP5. The resulting *in vitro* translation reaction was then incubated at 30 °C for 30 mins and stopped by the addition of 60 µM puromycin. Firefly luciferase activity was assayed using a Glomax 96 microplate illuminometer. The achieve this, 3 µl of translation reaction was added to 50 µl Bright-Glo Luciferase assay reagent (Promega) and

the resulting luminescence was measured in the illuminometer over a spectral wavelength of 350–650 nm and an integration time of 10 s at room temperature. After subtracting the background measured using an in vitro translation reaction to which no UTR-Luc mRNA had been added, the luminescence data were analyzed and plotted using the Origin 2018b software package. Each UTR-Luc mRNA was translated three times, and the mean and standard deviation of the luminescence data reported. Standard deviation reported is for variation of the mean for data obtained from a single batch of lysate. The mean reported is the value from all batches of lysate. Three to five different rabbit reticulocyte lysates were used for each UTR-Luc mRNA assay. Because of variation in activity among manufacturer's lysate samples, the ΔN-4G1 or DAP5 enhancement varied as much a three-fold.

Acknowledgements
This study was supported by Susan G. Komen for the Cure Postdoctoral Fellowship PDF12231199 to SM; National Institutes of Health, NIH R01 GM 084288 to RLG; National Center for Advancing Translational Sciences 1UL1TR002384-01 Seed Project to DJG; and National Science Foundation MCB 1513737 to DJG.

References

1. Hinnebusch AG & Lorsch JR (2012) The mechanism of eukaryotic translation initiation: new insights and challenges. *Cold Spring Harb Perspect Biol* 4(10).
2. Jackson RJ, Hellen CU, & Pestova TV (2010) The mechanism of eukaryotic translation initiation and principles of its regulation. *Nat Rev Mol Cell Biol* 11(2):113-127.
3. Hinnebusch AG, Ivanov IP, & Sonenberg N (2016) Translational control by 5'-untranslated regions of eukaryotic mRNAs. *Science* 352(6292):1413-1416.
4. Dennis MD, Shenberger JS, Stanley BA, Kimball SR, & Jefferson LS (2013) Hyperglycemia mediates a shift from cap-dependent to cap-independent translation via a 4E-BP1-dependent mechanism. *Diabetes* 62(7):2204-2214.
5. Silvera D*, et al.* (2009) Essential role for eIF4GI overexpression in the pathogenesis of inflammatory breast cancer. *Nat Cell Biol* 11(7):903-908.
6. Dhungel N*, et al.* (2015) Parkinson's disease genes VPS35 and EIF4G1 interact genetically and converge on alpha-synuclein. *Neuron* 85(1):76-87.
7. Dyer J & Sossin WS (2013) Characterization of the role of eIF4G in stimulating cap- and IRES-dependent translation in aplysia neurons. *PLoS One* 8(9):e74085.
8. Olszewska DA, McCarthy A, & Lynch T (2016) Commentary: Parkinson's Disease Genes VPS35 and EIF4G1 Interact Genetically and Converge on alpha-Synuclein. *Front Neurosci* 10:162.
9. Schrufer TL*, et al.* (2010) Ablation of 4E-BP1/2 prevents hyperglycemia-mediated induction of VEGF expression in the rodent retina and in Muller cells in culture. *Diabetes* 59(9):2107-2116.
10. Graber TE & Holcik M (2007) Cap-independent regulation of gene expression in apoptosis. *Mol Biosyst* 3(12):825-834.
11. Komar AA & Hatzoglou M (2011) Cellular IRES-mediated translation: the war of ITAFs in pathophysiological states. *Cell Cycle* 10(2):229-240.
12. Liberman N*, et al.* (2015) DAP5 associates with eIF2beta and eIF4AI to promote Internal Ribosome Entry Site driven translation. *Nucleic Acids Res* 43(7):3764-3775.
13. Plank TD & Kieft JS (2012) The structures of nonprotein-coding RNAs that drive internal ribosome entry site function. *Wiley Interdiscip Rev RNA* 3(2):195-212.
14. Braunstein S*, et al.* (2007) A hypoxia-controlled cap-dependent to cap-independent translation switch in breast cancer. *Mol Cell* 28(3):501-512.
15. Silvera D, Formenti SC, & Schneider RJ (2010) Translational control in cancer. *Nat Rev Cancer* 10(4):254-266.

16. Svitkin YV*, et al.* (2005) Eukaryotic translation initiation factor 4E availability controls the switch between cap-dependent and internal ribosomal entry site-mediated translation. *Mol Cell Biol* 25(23):10556-10565.
17. Alard A, Musa F, & Schneider R (2015) Evidence that the translational initiation factor DAP5 plays a critical role in breast cancer metastasis. *Cancer Res* 75.
18. Lee SH & McCormick F (2006) p97/DAP5 is a ribosome-associated factor that facilitates protein synthesis and cell proliferation by modulating the synthesis of cell cycle proteins. *EMBO J* 25(17):4008-4019.
19. Imataka H, Olsen HS, & Sonenberg N (1997) A new translational regulator with homology to eukaryotic translation initiation factor 4G. *EMBO J* 16(4):817-825.
20. Marcotrigiano J*, et al.* (2001) A conserved HEAT domain within eIF4G directs assembly of the translation initiation machinery. *Mol Cell* 7(1):193-203.
21. Weingarten-Gabbay S*, et al.* (2014) The translation initiation factor DAP5 promotes IRES-driven translation of p53 mRNA. *Oncogene* 33(5):611-618.
22. Khan MA*, et al.* (2014) Rapid kinetics of iron responsive element (IRE) RNA/iron regulatory protein 1 and IRE-RNA/eIF4F complexes respond differently to metal ions. *Nucleic Acids Res* 42(10):6567-6577.
23. Ma J*, et al.* (2012) Fe2+ binds iron responsive element-RNA, selectively changing protein-binding affinities and regulating mRNA repression and activation. *Proc Natl Acad Sci U S A* 109(22):8417-8422.
24. Lomakin IB, Hellen CU, & Pestova TV (2000) Physical association of eukaryotic initiation factor 4G (eIF4G) with eIF4A strongly enhances binding of eIF4G to the internal ribosomal entry site of encephalomyocarditis virus and is required for internal initiation of translation. *Mol Cell Biol* 20(16):6019-6029.
25. Dmitriev SE, Terenin IM, Dunaevsky YE, Merrick WC, & Shatsky IN (2003) Assembly of 48S translation initiation complexes from purified components with mRNAs that have some base pairing within their 5' untranslated regions. *Mol Cell Biol* 23(24):8925-8933.
26. Virgili G*, et al.* (2013) Structural analysis of the DAP5 MIF4G domain and its interaction with eIF4A. *Structure* 21(4):517-527.
27. Terenin IM, Smirnova VV, Andreev DE, Dmitriev SE, & Shatsky IN (2017) A researcher's guide to the galaxy of IRESs. *Cell Mol Life Sci* 74(8):1431-1455.
28. Filbin ME & Kieft JS (2009) Toward a structural understanding of IRES RNA function. *Curr Opin Struc Biol* 19(3):267-276.
29. Simon AE & Miller WA (2013) 3' cap-independent translation enhancers of plant viruses. *Annu Rev Microbiol* 67:21-42.
30. Lee AS, Kranzusch PJ, Doudna JA, & Cate JH (2016) eIF3d is an mRNA cap-binding protein that is required for specialized translation initiation. *Nature* 536(7614):96-99.
31. Lee AS, Kranzusch PJ, & Cate JH (2015) eIF3 targets cell-proliferation messenger RNAs for translational activation or repression. *Nature* 522(7554):111-114.
32. de la Parra C*, et al.* (2018) A widespread alternate form of cap-dependent mRNA translation initiation. *Nat Commun* 9(1):3068.
33. Coots RA*, et al.* (2017) m(6)A Facilitates eIF4F-Independent mRNA Translation. *Mol Cell* 68(3):504-514 e507.
34. Meyer KD*, et al.* (2015) 5' UTR m(6)A Promotes Cap-Independent Translation. *Cell* 163(4):999-1010.
35. Zhou J*, et al.* (2015) Dynamic m(6)A mRNA methylation directs translational control of heat shock response. *Nature* 526(7574):591-594.
36. Lee KM, Chen CJ, & Shih SR (2017) Regulation Mechanisms of Viral IRES-Driven Translation. *Trends Microbiol* 25(7):546-561.
37. Filbin ME & Kieft JS (2016) Linking Alpha to Omega: diverse and dynamic RNA-based mechanisms to regulate gene expression by 5'-to-3' communication. *F1000Res* 5.

38. Chen J & Kastan MB (2010) 5'-3'-UTR interactions regulate p53 mRNA translation and provide a target for modulating p53 induction after DNA damage. *Genes Dev* 24(19):2146-2156.
39. Sharma SD, Kraft JJ, Miller WA, & Goss DJ (2015) Recruitment of the 40S ribosome subunit to the 3'-untranslated region (UTR) of a viral mRNA, via the eIF4 complex, facilitates cap-independent translation. *J Biol Chem* 290(18):11268-11281.
40. Yasuda M, Hatanaka T, Shirato H, & Nishioka T (2014) Cell type-specific reciprocal regulation of HIF1A gene expression is dependent on 5'- and 3'-UTRs. *Biochem Biophys Res Commun* 447(4):638-643.
41. Chen TM*, et al.* (2014) Overexpression of FGF9 in colon cancer cells is mediated by hypoxia-induced translational activation. *Nucleic Acids Res* 42(5):2932-2944.
42. Ray PS, Grover R, & Das S (2006) Two internal ribosome entry sites mediate the translation of p53 isoforms. *EMBO Rep* 7(4):404-410.
43. Pestova TV, Hellen CU, & Shatsky IN (1996) Canonical eukaryotic initiation factors determine initiation of translation by internal ribosomal entry. *Mol Cell Biol* 16(12):6859-6869.
44. Avanzino BC, Fuchs G, & Fraser CS (2017) Cellular cap-binding protein, eIF4E, promotes picornavirus genome restructuring and translation. *Proc Natl Acad Sci U S A* 114(36):9611-9616.
45. Ozes AR, Feoktistova K, Avanzino BC, & Fraser CS (2011) Duplex unwinding and ATPase activities of the DEAD-box helicase eIF4A are coupled by eIF4G and eIF4B. *J Mol Biol* 412(4):674-687.
46. Treder K*, et al.* (2008) The 3' cap-independent translation element of Barley yellow dwarf virus binds eIF4F via the eIF4G subunit to initiate translation. *RNA* 14(1):134-147.

Figure Legends

Figure 1: A. cartoon of fluorescence anisotropy-based equilibrium binding assay **B.** Cartoon representation of omain architecture of full-length eIF4G1 and DAP5. Highlighted box depicts ΔN-4G1 truncation used in this study.

Figure 2: Equilibrium binding titrations of CITE-UTRs with ΔN-4G1 and DAP5. Normalized anisotropy changes for the interaction of fluorescein-labeled FGF-9 (-■-), HIF-1α (-▼-), $p53_A$ (-●-) and $p53_B$ (-♦-), with **A**. ΔN-4G1 and **B.** DAP5. 100 nM of fluorescein-labeled CITE-UTR in Titration Buffer was titrated with increasing concentrations of ΔN-4G1 or DAP5 at 25 °C and the anisotropy at each titration point was measured using excitation and emission wavelengths were 495 nm and 520 nm, respectively. Data points correspond to the average of three anisotropy measurements and the curves represent the non-linear fits that were used to obtain the averages and standard deviations for the corresponding K_d values.

Figure 3. Equilibrium binding titrations of EMCV J/K IRES and polyUC with ΔN-4G1 and DAP5. Normalized anisotropy changes for the interaction of fluorescein-labeled EMCV J/K IRES and poly UC with ΔN-4G1(-▼- and -∇-, respectively) and with DAP5 (-●- and -o-, respectively). Data were collected and analyzed as described in Fig. 2.

Figure 4. Effect of ΔN-4G1 and DAP5 on the expression of UTR-Luc mRNAs. **A.** Structure of the UTR-Luc mRNA reporter constructs containing a CITE-UTR upstream of the firefly luciferase gene with restriction enzyme sites indicated**.** The effect of increasing concentrations of **B.** ΔN-4G1 or **C.** DAP5 on the translation yields of HIF-1α, FGF-9, $p53_A$ and $p53_B$ UTR-Luc-mRNAs activity. UTR-Luc mRNAs were translated in rabbit reticulocyte lysate and relative luciferase activity measured in the absence (Bar Set 1) or presence (Bar Sets 2-8) of 0.2 mM m7G(5')ppp(5')G cap analog and in the absence (Bar Set 1) or presence (Bar Sets 2-8) of increasing concentrations of ΔN-4G1 or DAP5 added over the endogenous amount of eIF4G1 and DAP5 present in the rabbit reticulocyte lysate. Relative luciferase activity was normalized to the control reactions performed in the absence of m7G(5')pppp(5')G cap analog and added ΔN-4G1 or DAP5 (Bar Set 1 in B and C). Bar heights and error bars correspond to the average and standard deviations, respectively, of three relative luciferase activity measurements. ΔN-4G1 or DAP5-dependent stimulation of translation across experiments performed using different batches of rabbit reticulocyte lysate varied ~3-fold and t-tests using the average and standard deviation of all experiments exhibited a $p \leq 0.05$.

Supplementary Figure. 1. Titration of ΔN-4G1(-▼-) and DAP5 (-●-) to fluorescein labelled Ferritin IRE. Fluorescently labelled β-actin binding to ΔN-4G1 (-∇-) and DAP5 (-o-). Average of 3 independent experiments were performed data were collected and analyzed as Fig. 2.

Supplementary Figure. 2. Relative luciferase activity of uncapped β-actin mRNA reporter. ΔN-4G1 (A) or DAP5 (B) did not stimulates translation of the reporter RNA in rabbit reticulocytes lysates. Average of 3 independent experiments were performed and normalized luciferase activity ± S.D. calculated. Relative luciferase activity were calculated with normalization to control reactions performed in the absence of the cap analog or added ΔN-4G1 or DAP5.

A.

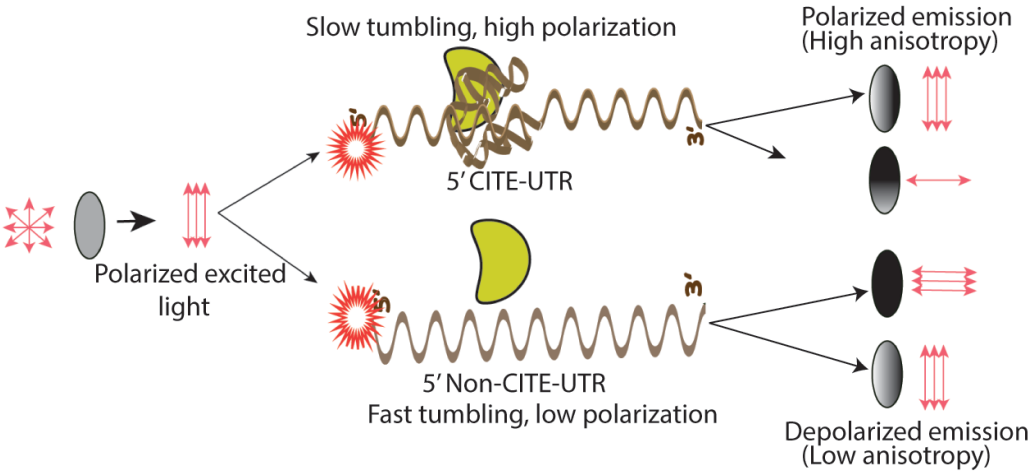

B.

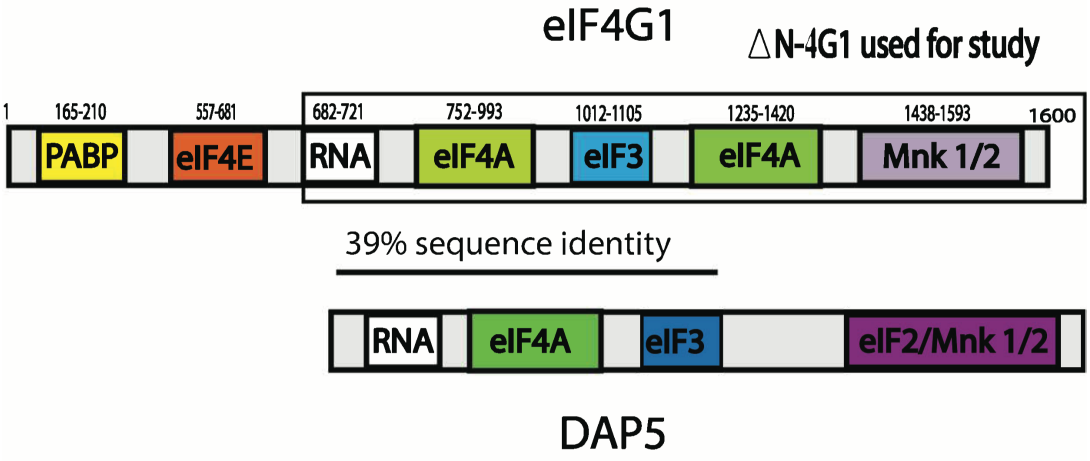

Figure 1

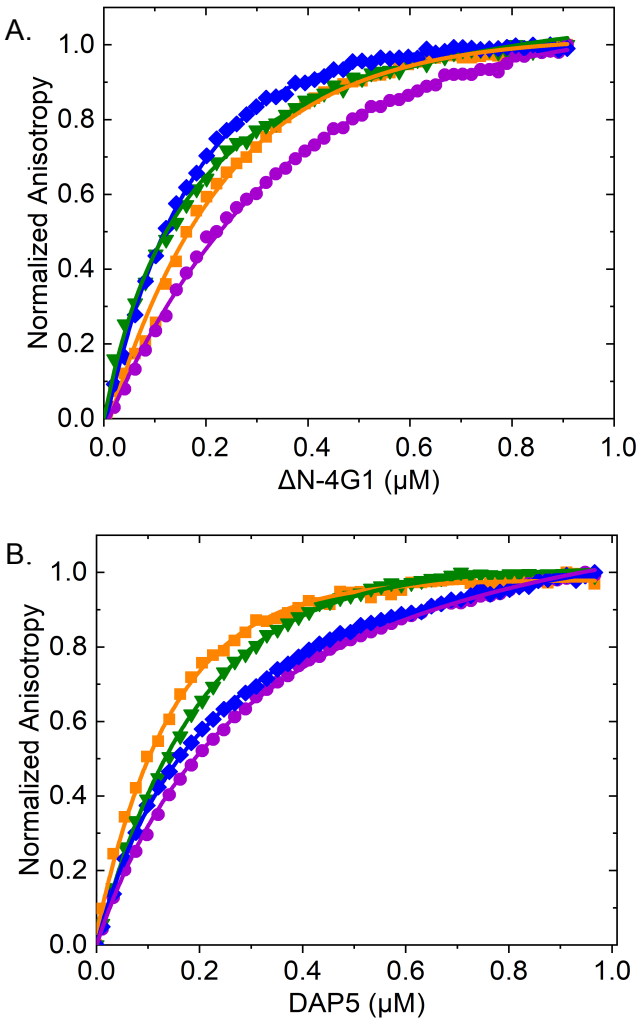

Figure 2

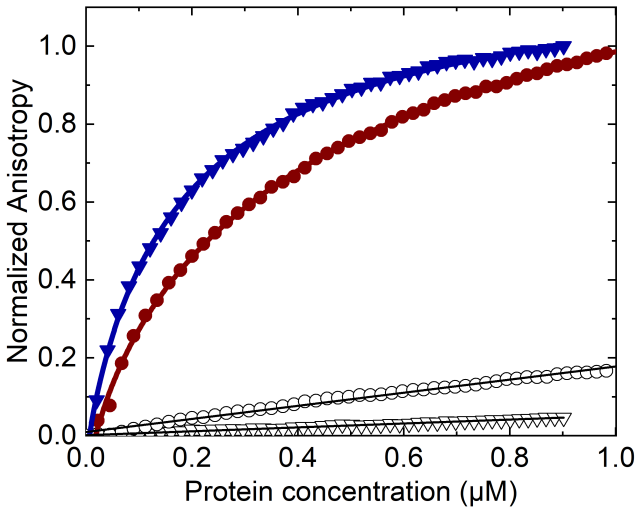

Figure 3

A.

B.

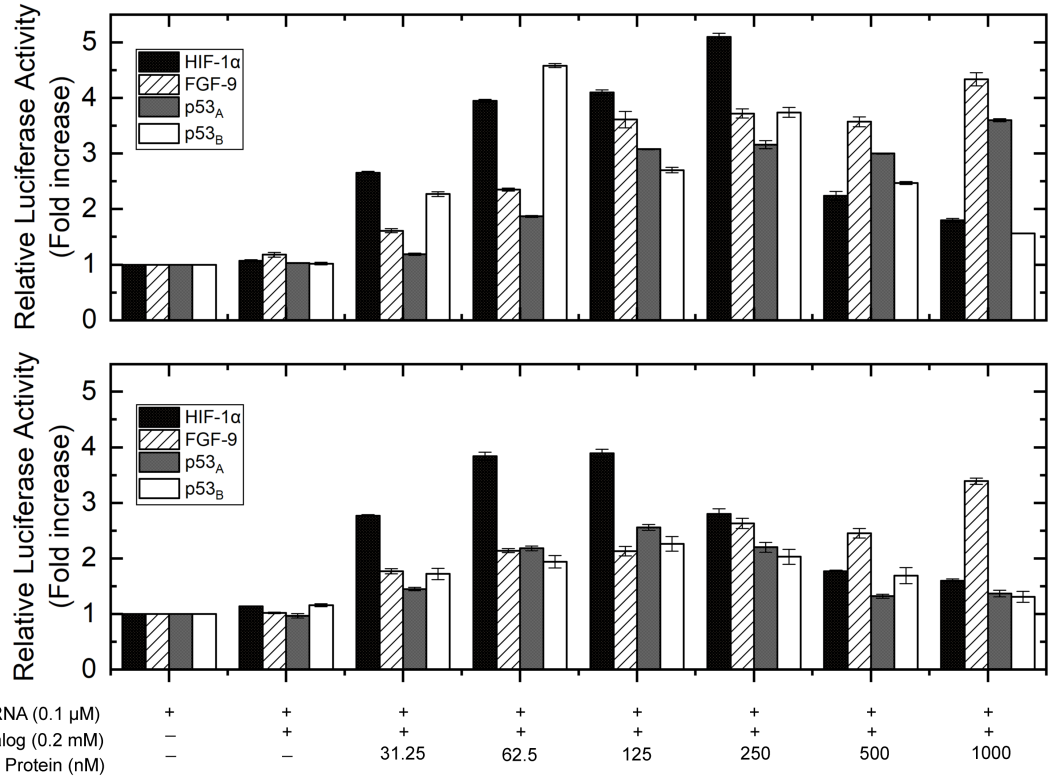

C.

RNA (0.1 μM)	+	+	+	+	+	+	+	+
Cap analog (0.2 mM)	–	+	+	+	+	+	+	+
Protein (nM)	–	–	31.25	62.5	125	250	500	1000

Figure 4

Table 1. Parameters describing the equilibrium binding of ΔN-4G1 and DAP5 to CITE-UTRs

CITE-UTRs	ΔN-4G1			DAP5		
	K_ds ± S.D. (nM)	Amplitudes (r_{max}-r_{min})	Goodness of fit (χ^2)	K_ds ± S.D. (nM)	Amplitudes (r_{max}-r_{min})	Goodness of fit (χ^2)
HIF-1α	165 ± 6.0	0.023	0.9934	172 ± 4.0	0.032	0.9960
FGF-9	183 ± 2.4	0.027	0.9959	102 ± 0.4	0.039	0.9971
$p53_A$	300 ± 1.0	0.036	0.9989	290 ± 1.0	0.044	0.9996
$p53_B$	126 ± 1.0	0.017	0.9983	234 ± 4.0	0.047	0.9975

Table 2. Parameters describing the effects of increasing concentrations of ΔN-4G1 and DAP5 on the translation of CITE-Luc mRNAs

CITE-Luc mRNAs	Maximum fold-increase	
	ΔN-4G1	DAP5
HIF-1α	5.1 ± 0.06	3.9 ± 0.07
FGF-9	4.3 ± 0.12	3.4 ± 0.06
$p53_A$	3.6 ± 0.03	2.6 ± 0.05
$p53_B$	4.6 ± 0.03	2.3 ± 0.13
β-actin	1.3 ± 0.04	1.2 ± 0.05

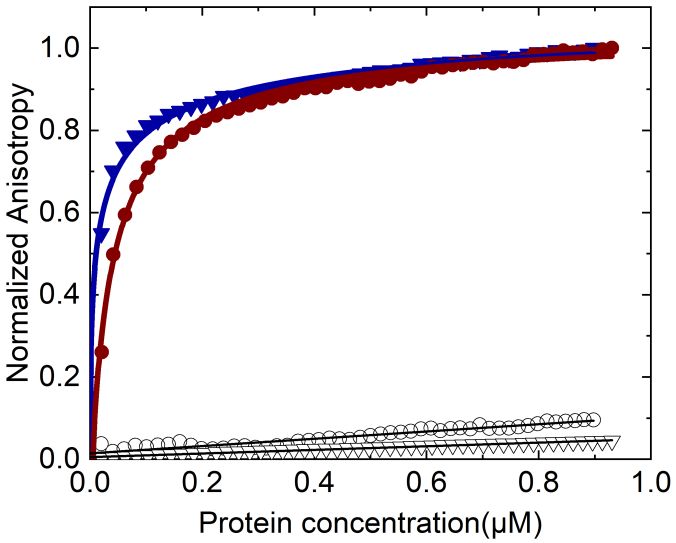

Supplementary Figure 1

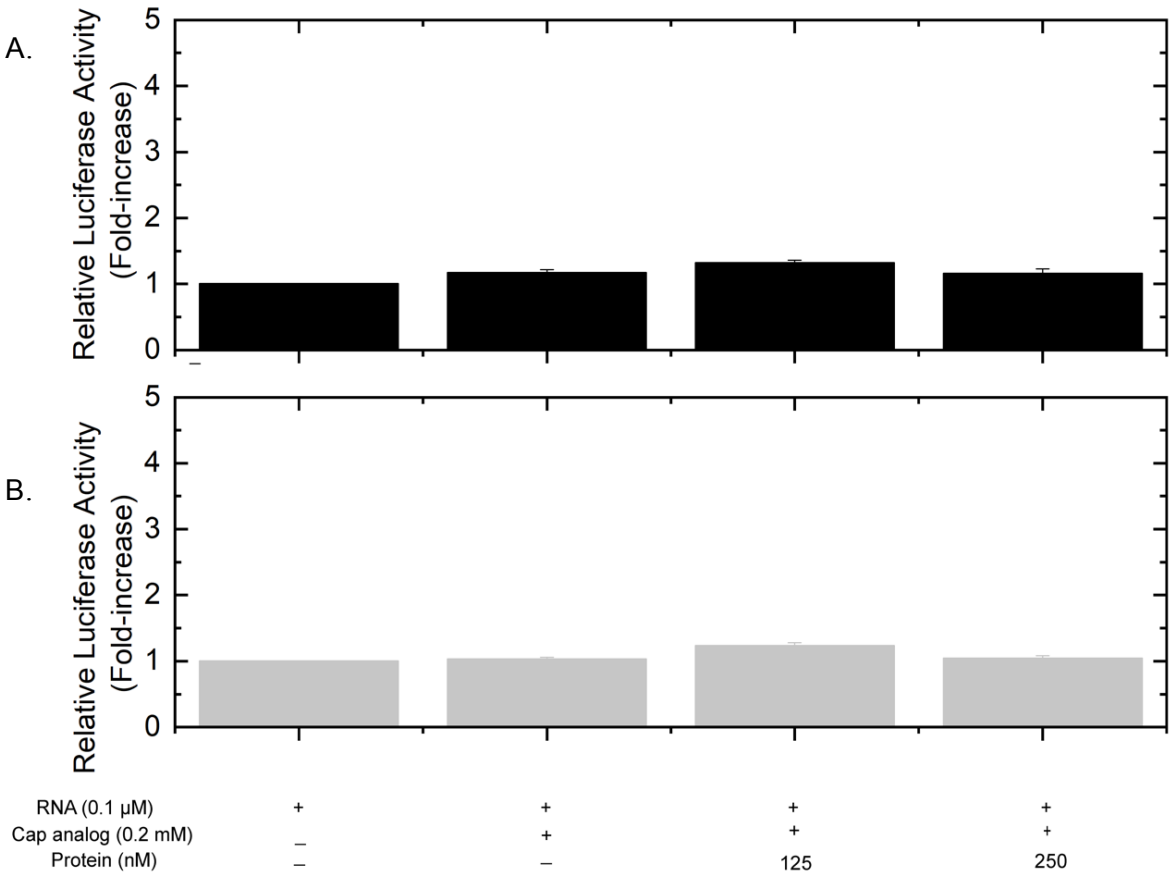

Supplementary Figure 2

Table S1. Parameters describing the equilibrium binding of ΔN-4G1 and DAP5 to Control UTRs

Control UTRs	ΔN-4G1			DAP5		
	K_ds ± S.D. (nM)	Amplitudes (r_{max}-r_{min})	Goodness of fit (χ^2)	K_ds ± S.D. (nM)	Amplitudes (r_{max}-r_{min})	Goodness of fit (χ^2)
EMCV J/K IRES	175 ± 4.0	0.031	0.9979	519 ± 21	0.045	0.9937
PolyUC	N. A	0.003	0.9973	N. A	0.010	0.9858
Ferritin IRE	18 ± 1.0	0.076	0.9940	35 ± 3.0	0.069	0.9996
β-actin	N. A	0.006	0.9107	N. A	0.039	0.9855